

Robust Market Making Under Model Uncertainty: The Role of Ambiguity Aversion and Competition

Harrison Lam, Guillem Ribas, Sergio Leal

March 15, 2025

Abstract

In the context of high-frequency trading markets, liquidity providers often work with imprecise models and must adjust their market-making decisions to remain competitive under a misspecified model. This work highlights the framework for a robust model and evaluates the performance of the optimal strategy under different market dynamics, exploring how market maker competition affects the Sharpe ratio of the trading strategy. We extend previous approaches by incorporating competitive effects among market makers, which significantly alters the impact of ambiguity aversion on the optimal quoting strategy. Our findings suggest that in a competitive setting, ambiguity aversion has a more subtle effect, particularly on the relationship between market share, execution risk, and profitability.

1 Introduction

In this report, we explore how market makers (MMs) attempt to maximize the profit in the spread they charge investors when providing liquidity to the market via buy and sell quotes. A common assumption in the market dynamics is that MMs have total knowledge of the stochastic processes that govern the optimal trades in and out of risky positions. Often, this assumption cannot be fully justified, as the model that MMs use may be incorrectly specified, causing the optimal trading decisions in this model to be less profitable in the real market environment.

Motivated by this problem, the work in [2] presents a robust framework that accounts for the MM model being misspecified. To do so, the case where the MM is completely certain of its model is considered first. Its objective is to maximize the expected profits of their strategy using the model given by

$$\sup_{\gamma \in A} \mathbb{E}^{\mathbb{P}}[f(\theta)], \quad (1)$$

with $f(\theta)$ defined as the function of profits depending on the variables, θ in the model, A defined as the set of possible strategies to follow, and \mathbb{P} corresponding to the reference measure of the model. When the MM is uncertain about its model (in the reference measure \mathbb{P}), it will look to improve its performance by introducing other possible models in a measure \mathbb{Q} . In order to choose one of these, Equation (1) is altered by introducing a penalization function, $\mathcal{H}(\mathbb{Q}|\mathbb{P})$, designed to avoid \mathbb{Q} -models that greatly deviate from the reference \mathbb{P} -model and simultaneously capture how averse the MM is to ambiguity [6]. The resulting expression is thus given by

$$\sup_{\gamma \in A} \inf_{\mathbb{Q} \in \mathcal{Q}} \mathbb{E}^{\mathbb{Q}}[f(\theta) + \mathcal{H}(\mathbb{Q}|\mathbb{P})], \quad (2)$$

with \mathcal{Q} representing the set of all possible alternate models.

In Section 2 we define the reference \mathbb{P} -model and its associated variables. Using this and considering the space of alternate \mathbb{Q} -models, the system of ordinary differential equations (ODEs) is derived to find the optimal MM strategy under the reference and misspecification robust models. In Section 3 we reproduce the results in [2] and extend them by considering the presence of other MMs in the market, affecting the effectiveness of the MM's own optimal trading strategy. Finally, we provide our conclusion in Section 4.

2 Setting the scene

When specifying a reference model to choose the level at which to send limit orders (LOs) to the limit order book (LOB), the MM must provide a model for the following.

- **Mid-price:** The mid-price of the asset is assumed to satisfy the following SDE

$$dS_t = \alpha S_t + \sigma dW_t, \quad (3)$$

where $\alpha \in \mathbb{R}$, $\sigma > 0$ and the process $(W_t)_{0 \leq t \leq T}$ is a Brownian motion.

- **Limit Order Book:** The other MMs in the market post quotes to the LOB. Hence, the MM will model that the distances from the mid-price to the maximum or minimum execution price of a market order (MO) follow an exponential distribution with parameters κ^+ and κ^- , respectively. As a result, the probability that a given MO fills an LO of unit volume at distance y from the mid-price is given by

$$p^\pm(y) = e^{-\kappa^\pm y}, \quad (4)$$

since LOs are only filled by MOs when the execution price is greater than that of the LO.

- **Market Orders:** Liquidity-taking market participants are modeled to send MOs following Poisson processes M_t^+ and M_t^- with corresponding parameters λ^+ and λ^- for sell and buy MOs, respectively.

In order to formally define the wealth process of the MM, independent Poisson random measures $\mu^\pm(dy, ds)$ are introduced to represent the counting processes for filled LOs, given by

$$N_t^\pm = \int_0^t \int_{\delta_s^\pm}^\infty \mu^\pm(dy, ds), \quad (5)$$

where δ_t^\pm are the processes corresponding to the depth around the mid-price of the quotes posted by the MM. Therefore, the process corresponding to the wealth of the MM, $(X_t)_{0 \leq t \leq T}$, follows the SDE

$$dX_t = (S_t + \delta_t^+)dN_t^+ - (S_t - \delta_t^-)dN_t^-, \quad (6)$$

by noting that the MM pays $S_t - \delta_t^-$ for a filled buy order and receives $S_t + \delta_t^+$ for a filled sell order. As a result, the inventory of the MM at a given time will be given by $q_t = N_t^- - N_t^+$.

Having specified the reference model, the expression in Equation (1) can be transformed into the value function H , defined as

$$H(t, x, q, S) = \sup_{(\delta_s^\pm)_{t \leq s \leq T} \in A} \mathbb{E}^\mathbb{P}[X_T + q_T(S_T - \ell(q_T)) | X_t = x, q_t = q, S_t = S], \quad (7)$$

where T is the end time of the strategy and $\ell(q)$ is an increasing function in q acting as a position liquidation penalty corresponding to market fees and market impact costs when the MM sends an MO to unwind their position at time T . It is also important to note that, in practice, the MM will have capital constraints, preventing it from building large positions. To enforce this, the values of q_t are restricted so that $\underline{q} \leq q_t \leq \bar{q}$ for some finite $\underline{q}, \bar{q} \in \mathbb{Z}$.

The solution to Equation (7) can be reformulated as a system of ODEs [2] of the form

$$\begin{aligned} \partial_t H + \alpha \partial_S H + \frac{1}{2} \sigma^2 \partial_{SS} H + \sup_{\delta^+ \geq 0} \{ \lambda^+ e^{-\kappa^+ \delta^+} (H(t, x + (S + \delta^+), q - 1, S) - H(t, x, q, S)) \} \\ + \sup_{\delta^- \geq 0} \{ \lambda^- e^{-\kappa^- \delta^-} (H(t, x + (S - \delta^-), q + 1, S) - H(t, x, q, S)) \} = 0. \end{aligned} \quad (8)$$

with terminal condition $H(T, x, q, S) = x + q(S - \ell(q))$. Considering the ansatz, $H(t, x, q, S) = x + qS + h_q(t)$, the optimal values for δ^+ and δ^- are then calculated in [2] to be

$$\begin{aligned} \delta_t^{+*}(t) &= \left(\frac{1}{\kappa^+} - h_{q-1}(t) + h_q(t) \right)^+, \quad q \neq \underline{q}, \\ \delta_t^{-*}(t) &= \left(\frac{1}{\kappa^-} - h_{q-1}(t) + h_q(t) \right)^+, \quad q \neq \bar{q}. \end{aligned} \quad (9)$$

Nevertheless, in practice, the MM will never be completely certain that its model exactly captures the dynamics of the market. Knowing this, it will consider alternative models over equivalent measures, \mathbb{Q} . This is done by adding a term to Equation (7) that acts as a cost function for rejecting the \mathbb{P} reference model in favor of a \mathbb{Q} candidate model. This is formulated as

$$H(t, x, q, S) = \sup_{(\delta_s^\pm)_{t \leq s \leq T} \in A} \inf_{\mathbb{Q} \in \mathcal{Q}} \mathbb{E}^{\mathbb{Q}}[X_T + q_T(S_T - \ell(q_T)) + \mathcal{H}(\mathbb{Q}^{\alpha, \lambda, \kappa}(\eta, g) | \mathbb{P}) | X_t = x, q_t = q, S_t = S], \quad (10)$$

with η representing the mid-price drift under the new measure and g representing the shift in intensity of the Poisson processes modeling the MO arrivals. Again, under the ansatz, $H(t, x, q, S) = x + qS + h_q(t)$, the solution to the equation follows a system of ODEs [2] given by

$$\begin{aligned} \partial_t h_q + \alpha q - \frac{1}{2} \phi_\alpha \sigma^2 q^2 \\ + \frac{\lambda^+}{\phi_\lambda} \left(1 - \exp \left(\frac{\phi_\lambda}{\phi_\kappa} \log(1 - e^{-\kappa^+ \delta^{+*}} + e^{-\kappa^+ \delta^{+*} - \phi_\kappa(\delta^{+*} + h_{q-1} - h_q)}) \right) \right) \mathbb{I}_{q \neq \underline{q}} \\ + \frac{\lambda^-}{\phi_\lambda} \left(1 - \exp \left(\frac{\phi_\lambda}{\phi_\kappa} \log(1 - e^{-\kappa^- \delta^{-*}} + e^{-\kappa^- \delta^{-*} - \phi_\kappa(\delta^{-*} + h_{q-1} - h_q)}) \right) \right) \mathbb{I}_{q \neq \bar{q}} = 0, \end{aligned} \quad (11)$$

with boundary condition $h_q(T) = -q\ell(q)$. Note that the parameters $\phi_\alpha, \phi_\lambda$ and ϕ_κ represent how uncertain the MM is on the values of α, λ^\pm and κ^\pm in its model, with larger values representing higher uncertainty. As a result of this, the cost function $\mathcal{H}(\mathbb{Q}^{\alpha, \lambda, \kappa}(\eta, g) | \mathbb{P})$ will yield a lower cost when the MM has a higher degree of uncertainty. Additionally, due to this added uncertainty, the optimal values for δ^+ and δ^- are now shown [2] to be

$$\begin{aligned} \delta_q^{+*}(t) &= \left(\frac{1}{\phi_\kappa} \log \left(1 + \frac{\phi_\kappa}{\kappa^+} \right) - h_{q-1}(t) + h_q(t) \right)^+, \quad q \neq \underline{q}, \\ \delta_q^{-*}(t) &= \left(\frac{1}{\phi_\kappa} \log \left(1 + \frac{\phi_\kappa}{\kappa^-} \right) - h_{q-1}(t) + h_q(t) \right)^+, \quad q \neq \bar{q}. \end{aligned} \quad (12)$$

3 Validation of the Robust Market-Making Model

For the reproducibility of the results, we used an explicit finite-difference scheme with

$$\partial_t h_q \approx \frac{h_q(t) - h_q(t - \Delta t)}{\Delta t}$$

to find an approximate solution to the system of ODEs outlined in Equation (11).

3.1 Impact of Individual Ambiguity Factors

We start by analyzing the effects of each type of ambiguity individually. Setting the other two parameters to zero makes this possible. We begin with setting $\phi_\lambda = \phi_\kappa = 0$, and focusing on the uncertainty of the MM with respect to the mid-price drift, which can be due to multiple causes, such as using an unsophisticated model for it or not having enough information to estimate it. For this particular case, we make use of Proposition 5 in [2], which provides an exact analytical solution for $h_q(t)$.

In Figure 1, we observe that when drift uncertainty increases and inventory q is positive, the optimal sales depths are smaller, reaching almost zero when $\phi_\alpha = 100$. The opposite behavior is observed when the MM is short, hence the optimal strategy is to close positions faster when drift uncertainty is large. Another important fact that the authors note is that the new optimal drift for the mid-price, η_q^* , which is no longer constant, only depends on the volatility σ when $\phi_\alpha \neq 0$. The graph on the right shows that the total depth increases with ϕ_α , allowing the MM to offset their losses from trading with better-informed participants.

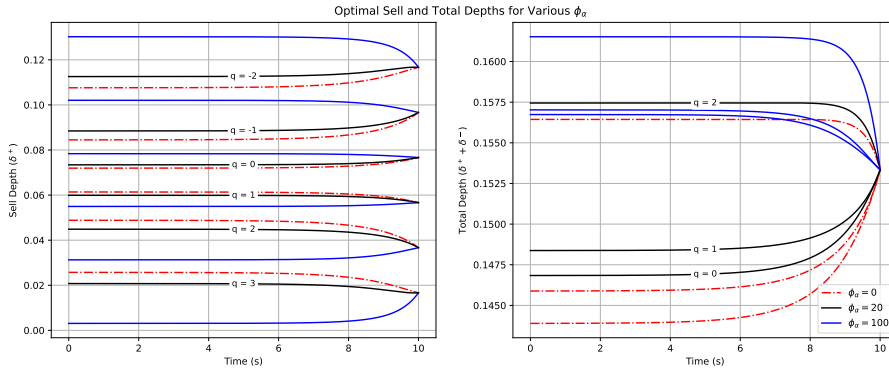


Figure 1: Optimal sell and total depth under ambiguity aversion to midprice drift. Other parameter values are $\kappa^\pm = 15$, $\lambda^\pm = 2$, $\sigma = 0.01$, $\alpha = 0$, $\ell(q) = \theta q$, $\theta = 0.01$, $\bar{q} = -q = 3$ and $T = 10$ s.

Next, we focus on the uncertainty of the arrival intensity of market orders, setting $\phi_\alpha = \phi_\kappa = 0$. In an environment where the rate of arrival is uncertain, the market maker requires more compensation for the risk of not being able to close their position. This is consistent with the result shown in the graph on the right of Figure 2, with the optimal total depths being wider. The graph on the left displays behaviour similar to the previous case, with quicker mean reversion to optimal inventory levels for larger ambiguity aversion.

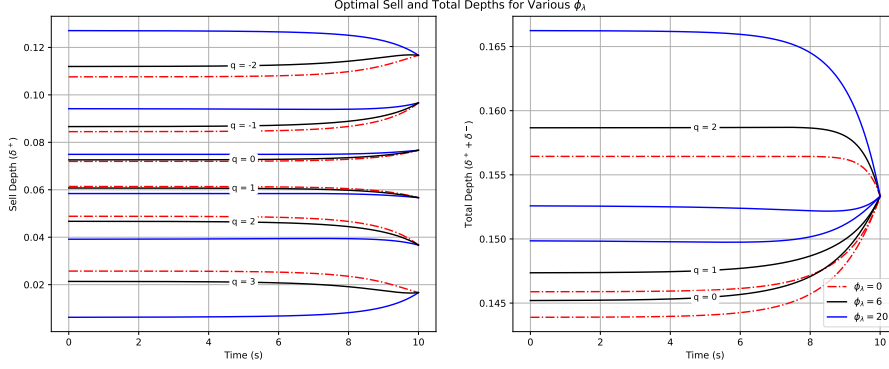


Figure 2: Optimal sell and total depth under ambiguity aversion to MO fill probabilities. Other parameter values are $\kappa^\pm = 15$, $\lambda^\pm = 2$, $\sigma = 0.01$, $\alpha = 0$, $\ell(q) = \theta q$, $\theta = 0.01$, $\bar{q} = -q = 3$ and $T = 10$ s.

Finally, we consider the case where the MM is ambiguity averse to the fill probabilities of LOs, keeping the other ambiguity parameters equal to zero. In contrast to the previous two cases, when ϕ_κ increases, the MM posts prices closer to the mid-price, as shown in Figure 3. Concerned that the posted LOs may not be executed, the MM decreases their LO spread to gain market share at the expense of lowering the profit per trade.

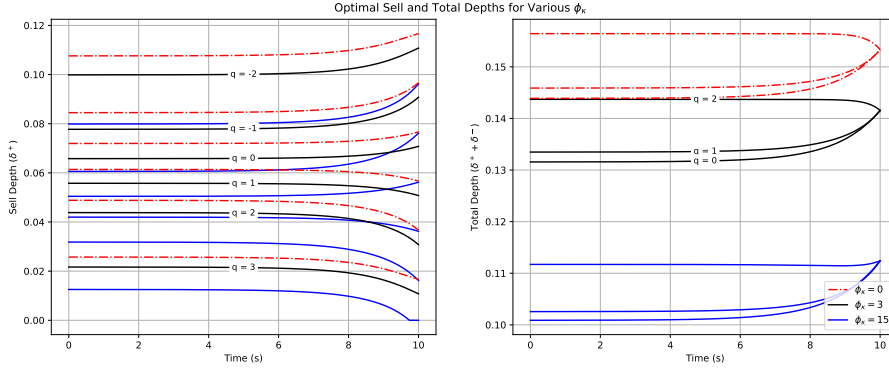


Figure 3: Optimal sell and total depth under ambiguity aversion to MO arrival rate. Other parameter values are $\kappa^\pm = 15$, $\lambda^\pm = 2$, $\sigma = 0.01$, $\alpha = 0$, $\ell(q) = \theta q$, $\theta = 0.01$, $\bar{q} = -q = 3$ and $T = 10$ s.

3.2 Effects of Joint Ambiguities on Optimal Strategies

In this section, we consider the case where all three ambiguity factors are non-zero. In the graph on the left of Figure 4, we observe that the optimal behaviour changes drastically depending on the set of ambiguity parameters. When the ambiguity is weighted more strongly towards the drift α and the arrival rate λ , the MM prioritises closing their position quickly, while for the other set of parameters, the MM posts tighter spreads to gain market share.

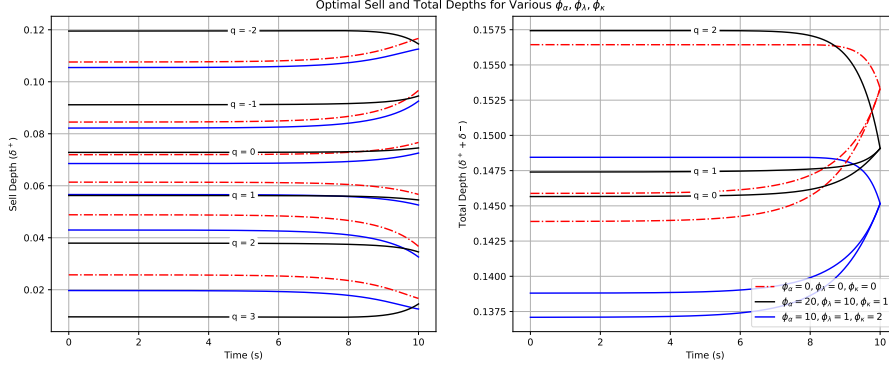


Figure 4: Optimal sell and total depths for MM that is ambiguity averse towards MO arrival rate, fill probabilities and midprice drift. Other parameter values are $\kappa^\pm = 15$, $\lambda^\pm = 2$, $\sigma = 0.01$, $\alpha = 0$, $\ell(q) = \theta q$, $\theta = 0.01$, $\bar{q} = -q = 3$ and $T = 10$ s.

The graph on the right of Figure 4 shows that for $\phi_\alpha = 20, \phi_\lambda = 10, \phi_\kappa = 1$, the total depths are wider than the ambiguity-neutral case until close to expiration, which as we discussed in Figures 1 and 2, helps the MM recover from adverse selection losses.

3.3 Profitability and Risk Analysis in Market Making

Having defined a robust model for the optimal trading decisions of the MM, we would like to quantify up to what extent the new model improves the MM's performance in relation to the previous possibly misspecified model.

3.3.1 Market Performance in a Non-Competitive Setting

In our initial simulation of the market model, we follow the approach described in [3], which defines the true dynamics of the market as

$$\begin{aligned}
 dS_t &= \alpha_t dt + \sigma dW_t, \\
 d\alpha_t &= -\beta_\alpha \alpha_t dt + \epsilon^+ dM_t^+ - \epsilon^- dM_t^-, \\
 d\lambda_t^\pm &= \beta_\lambda (\theta_\lambda - \lambda_t^\pm) dt + \eta_\lambda dM_t^\pm + \nu_\lambda dM_t^\mp, \\
 d\kappa_t^\pm &= \beta_\kappa (\theta_\kappa - \kappa_t^\pm) dt + \eta_\kappa dM_t^\pm + \nu_\kappa dM_t^\mp.
 \end{aligned} \tag{13}$$

It is important to note that the MM is, in part, ignorant to these dynamics, as it cannot fully know how the market works. The intensities of MO arrivals, λ_t^\pm , follow a Hawkes process, which captures the self-causality trait of trades commonly observed in real markets [5], while α_t captures the effect of temporary alpha caused by MOs. As for the LOB dynamics, the parameters κ_t^\pm are mean-reverting with jump processes representing the temporary effect of MOs on the LOB depth.

σ	ϵ^\pm	β_α	θ_λ	β_λ	η_λ	ν_λ	θ_κ	β_κ	η_κ	ν_κ
0.01	0.001	1	0.2	$\frac{70}{9}$	5	2	15	$\frac{7}{6}$	5	2

Table 1: Parameters used to generate market dynamics.

We reproduce the market simulation with the same parameters as [2], outlined in Table 1. We define our penalty function $\ell(q) = 0.001q$ and inventory constraints $\bar{q} = -\underline{q} = 8$ to calculate our

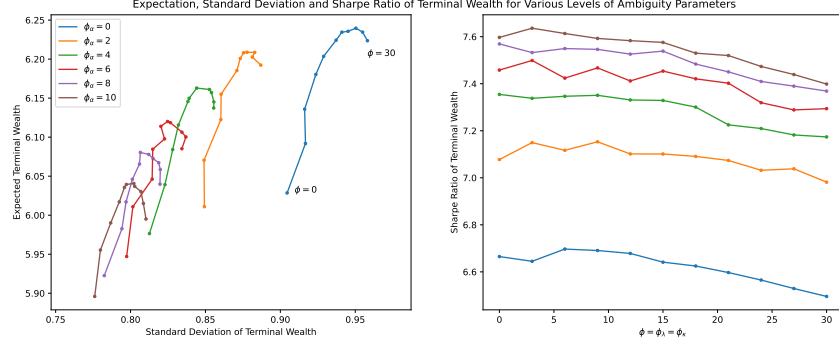


Figure 5: Expectation, standard deviation and Sharpe ratio of terminal wealth for various ambiguity parameters, 300 seconds of simulation.

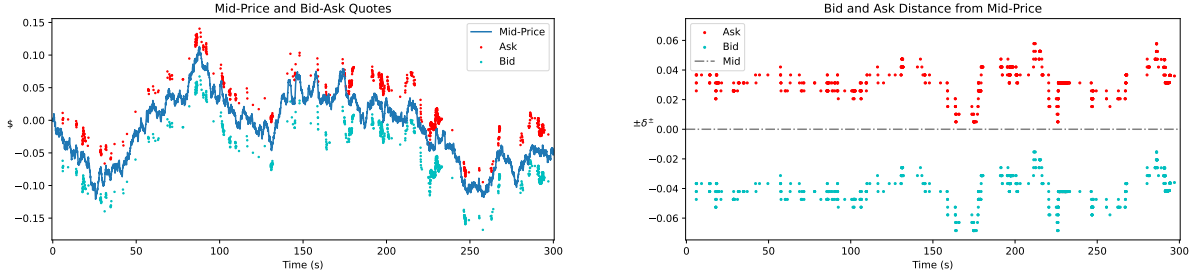


Figure 6: Bid-Ask quotes by the MM when MOs arrive and values of δ^+ and δ^- during time.

PnL, as in [2]. For the MM's reference model, we assume that they use constant parameters λ^\pm , κ^\pm and α , which they manage to calibrate through market observation, yielding the values $\lambda^\pm = 2$, $\kappa^\pm = 27$ and $\alpha = 0$.

To process the arrival of market orders (MOs), in every time interval of the discretization scheme, the intensities of buy and sell market orders, λ^+ and λ^- , are assumed to be constant, representing the expected arrival rates per unit time. Since order arrivals follow a Poisson process, the number of arrivals is almost surely (*a.s.*) 0 or 1 in an infinitesimal interval. However, in a discrete setting, ΔM_t^\pm could take values greater than 1. Therefore, when $\Delta M_t^+ + \Delta M_t^- > 1$, we make the simplifying assumption that they arrive uniformly across the discretisation grid in a random order.

The number of generated paths is $M = 30,000$, and we compute the Sharpe ratio as the quotient between the expected profit and its standard deviation across all paths. The uncertainty parameters are $\phi_\alpha \in \{0, 2, 4, 6, 8, 10\}$, $\phi_\lambda = \phi_\kappa = \phi \in \{0, 3, 6, 9, 12, 15, 18, 21, 24, 27, 30\}$. The graph on the right of Figure 5 shows that, with $\phi = \phi_\lambda = \phi_\kappa$ constant, the Sharpe ratio of the MM increases significantly with respect to the ambiguity aversion to mid-price drift, as a result of better management of inventory risks and lower adverse selection costs. This pattern is consistent with the result presented in the original paper, with the graph on the left showing an inverted smile for all values of ϕ_α .

The left-hand side of Figure 6 shows the market maker's LO quotes when MOs arrive, and the graph on the right shows the bid and ask distance from the mid-price. These distances are related to the graph on the left of Figure 7, which displays the market maker's inventory and the

intensities of the MO arrival processes M_t^\pm . The right-hand side of Figure 7 shows the market maker's wealth during the simulation (cash and mark-to-market), with a terminal adjustment of $ql(q)$. We note that this liquidation adjustment is negligible in magnitude compared to the wealth gained during trading. We repeat this simulation for a convex $l(q)$, which penalises large terminal inventories more. The Sharpe ratios obtained are still increasing in ϕ_α , but unlike the previous case, it is increasing and concave with respect to ϕ . We present these results in the Appendix.

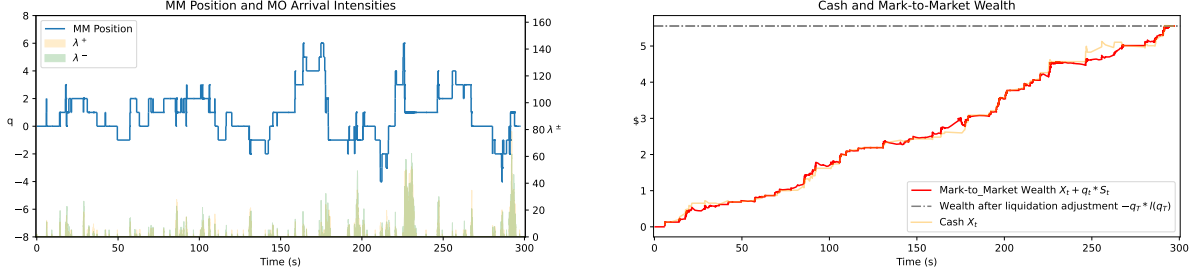


Figure 7: Inventory held by the MM, arrival intensities λ^+ and λ^- and cash and Mark-to-Market wealth of the MM including inventory penalty in the end.

3.3.2 Market Performance with Competition

When performing the market simulation as in [2], the lack of market competition becomes apparent, yielding unrealistic PnL and Sharpe ratios for 300 seconds of trading. In practice, there are multiple MMs operating in the market, and under the simplifying assumption that all LOs have unit volume, a key metric for an MM's performance is the proportion of its LOs being filled by the incoming MOs (market share). Given that the market is not perfectly competitive, a greater market share generally implies a greater expected profit for the MM. In turn, this generates a competitive effect where, upon seeing LOs being filled in the market, adversary MMs will tighten their spreads to try to maintain their market share. In this section, we will consider this extension to the previous market dynamics, which also considers the competition between MMs in addition to the market's reaction to the influx of MOs. Figure 8 illustrates the loss of market share of the MM and the exposure to market risk in the newly specified market dynamics, justifying the need to study the model's performance in this new environment.

To model this behaviour in the market model, we alter the SDE that defines the κ_t^\pm stochastic processes. Now, we have that

$$\begin{aligned} d\kappa_t^\pm &= \beta_\kappa(\theta_\kappa + \psi_t - \kappa_t^\pm) + \eta_\kappa dM_t^\pm + \nu_\kappa dM_t^\pm, \\ d\psi_t^\pm &= (\gamma - 1)\psi_t dt + \zeta^\pm dN_t^\pm. \end{aligned} \quad (14)$$

where N_t^\pm is the previously defined counting process of filled LOs.

Conceptually, the processes ψ_t^\pm are exponentially decaying processes that are bumped by the MM's LOs being filled. These processes are then added to the original mean reversion of the κ_t^\pm processes. This implies that, upon the MM's LOs being filled, competition occurs, causing an immediate increase in the mean reversion level of the market parameters κ^\pm . The exponential decay of ψ_t^\pm then corresponds to the relaxation of the competition, caused by the exit of market participants and competitor MMs wanting to avoid adverse selection. $\gamma = 0.799$ and $\zeta^\pm = 30$ were the parameters used to run the simulation under the revisited model, corresponding to a

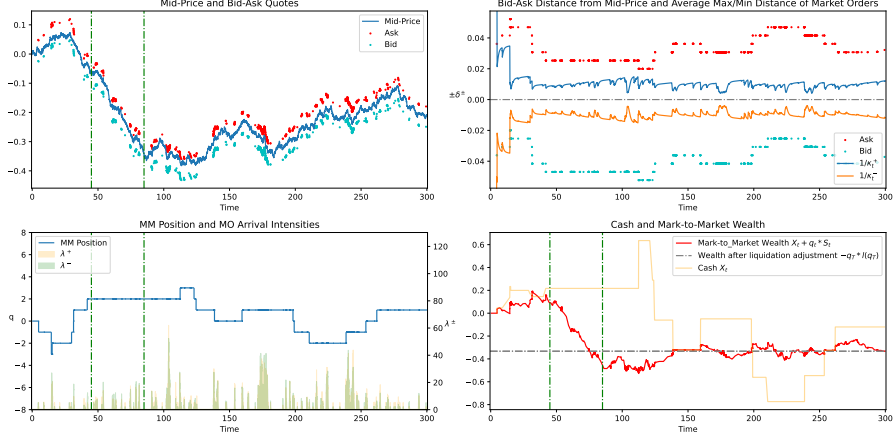


Figure 8: Results when not updating the quotes with respect to the market changes.

1% decay every 0.05 seconds.

In the initial implementation, our estimate of κ_t^\pm is kept constant at 27 throughout the entire trading period without recalibrating it to the market, assuming that the MM had calibrated their model to the long-term mean of κ_t^\pm before the trading session. Now, as the market is reactionary to the MM's trades, the long-term mean of κ_t^\pm will change upon the entry of the MM into the market. As a result, the MM's quote remains wider than the average maximum and minimum execution price of incoming buy and sell MOs, respectively. This decreases the number of trades and increases the MM's exposure to market and inventory risk. This phenomenon is illustrated in Figure 8, where, between $t = 45s$ and $t = 85s$ (indicated by the green dotted lines), the MM is stuck with a position of $q = 2$ (bottom left panel) and is unable to trade due to the depth of its quotes (top right panel). Consequently, it suffers from exposure to market risk, and as the mid-price S_t is decreasing (top left panel), it leads to a decline in its mark-to-market wealth (bottom right panel).

We also note that under these new dynamics, the value of κ_t^\pm spikes a lot more, causing the maximum/minimum execution price of MOs to be unrealistically close to the mid price, shown by the average distance $1/\kappa_t^\pm$ in the top right panel. Therefore, we introduce tick sizes (0.0025), in the model, where we round all MO and LO prices to the smallest tick size above to prevent the orders from being arbitrarily close to the mid-price.

In a more realistic setting, the MM will update its estimate of κ_t^\pm periodically every γ seconds to increase its participation in the market, as, upon market entry, it has altered the dynamics of the κ_t^\pm processes. These updates are based on the distances between the maximum/minimum execution prices of buy/sell MOs and the mid-price, which, under our model assumptions, follow an exponential distribution with parameters κ_t^\pm . To avoid overfitting to the observed samples, updates are performed only if there have been more than 10 MO arrivals since the last recalibration. Once this condition is met, κ_t^\pm is recalibrated to the reciprocal of the sample mean of the respective distances. $\gamma = 5$ has been chosen for this experiment, due to the fact that $\lambda^\pm = 2$ implies that on average, there will be 10 MOs (per side) every 5 seconds.

In the right panel of Figure 9, we observe a bump in κ^+ between $T = 40s$ and $T = 140s$, after which it almost reverts to its original value. The recalibration is reflected in the MM's estimated

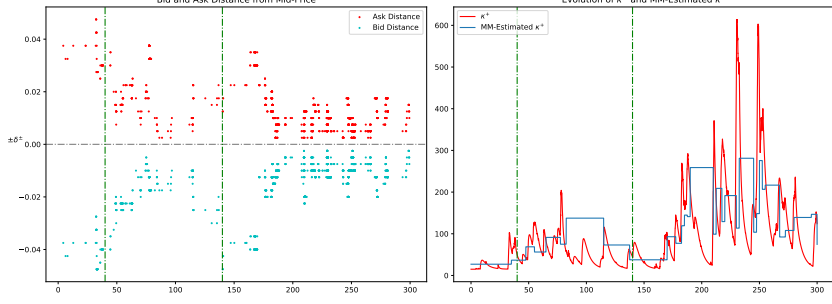


Figure 9: Results when updating the quotes with respect to the market changes.

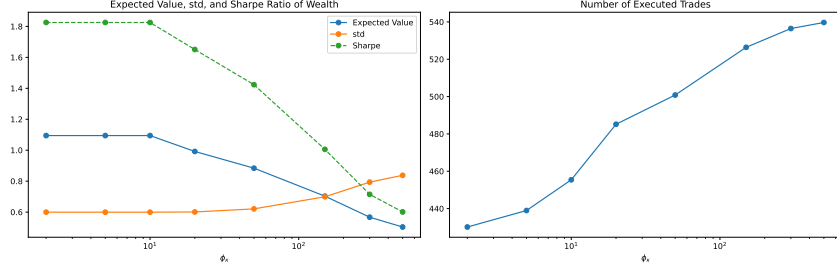


Figure 10: Expected value, std and Sharpe ratio of terminal wealth and average number of executed trades for $\phi_\kappa \in \{2, 5, 10, 20, 50, 150, 300, 500\}$.

κ^+ (shown in blue in the right panel), leading to adjustments in the quotes, as seen in the left panel. By responding to the initial increase in κ^+ , the MM maintains trading activity with a tighter spread, and as κ^+ decreases, the MM updates its estimate accordingly, widening the spread.

Under the new market dynamics, we observe that the ambiguity aversion parameter ϕ_κ has a much smaller impact on the MM's quotes, and hence market share. This is due to the newly introduced competition between MMs, which causes the MM to quote closer to the mid-price. As the MM spread is already very tight, it cannot decrease much further, unlike in the original case (Figure 3). The decrease in the profit per trade also offsets any potential profits gained from the increase in market share. This is shown in Figure 10, where the expected terminal wealth decreases with ϕ_κ , while the standard deviation increases slightly due to the larger number of trades executed. The decrease in Sharpe ratio is also observed in Figure 5, but in that case, it comes with an upside, as the expected terminal wealth increases. Hence, increasing the ambiguity aversion ϕ_κ no longer improves the MM's PnL in these new market dynamics.

4 Conclusion

In this report, we have shown how, by incorporating ambiguity in model choice, a MM can make their market model activities more robust to model misspecification. Following the framework introduced in [2], we have implemented a model that allows control of the levels of ambiguity for the different key market parameters α , λ , and κ . Under the market dynamics outlined in [3], we have reproduced the results obtained in [2], confirming the significant improvement in the MM's performance when using the model.

In revisiting the SDEs governing the κ_t^\pm processes, we have also considered a market with dy-

namics that more closely resemble real-world competition between market makers. Our results show that in a non-competitive setting, ambiguity aversion significantly improves the MM’s performance by mitigating adverse selection and inventory risks. However, in a competitive market, we find that ambiguity aversion has a diminishing effect as other market makers adjust their spreads in response. This suggests that ambiguity aversion alone may not be sufficient to optimize a market-making strategy in competitive environments, where market share dynamics play a dominant role in execution risk and profitability.

Given that ambiguity aversion has a limited effect in competitive environments, market makers might benefit more from strategies that dynamically adjust to order flow and competitor behavior, rather than relying only on robust modeling assumptions. This points to the need for adaptive execution models that can adjust quoting strategies based on real-time market conditions rather than static ambiguity adjustments.

A straightforward application of the current model to real markets, without assumptions on the stock dynamics (in particular, the arithmetic BM, which is unrealistic at a microstructure level), would involve observing the last traded price and using the uncertainty zones model to reconstruct the stock price. However, recalibration of the model parameters would be necessary to account for changes in market dynamics, especially λ_t^\pm , since it fluctuates considerably around the long-term average of $\lambda^\pm = 2$.

As an extension to the current model, one could also consider a non-constant volatility in the mid-price SDE [1], more closely resembling the dynamics observed in the market. Furthermore, a crucial assumption in this model is the posting of unit volume LOs. In practice, LOs vary in size, implying that a distinct LOB model [4] which includes the possibility of a partial LO fill, would yield more realistic results.

References

- [1] Burcu Aydoğan, Ömür Uğur, and Ümit Aksoy. “Optimal Limit Order Book Trading Strategies with stochastic volatility in the underlying asset”. In: *Computational Economics* 62.1 (June 2022), pp. 289–324. DOI: 10.1007/s10614-022-10272-4.
- [2] Álvaro Cartea, Ryan Donnelly, and Sebastian Jaimungal. “Algorithmic trading with model uncertainty”. In: *SIAM Journal on Financial Mathematics* 8.1 (Jan. 2017), pp. 635–671. DOI: 10.1137/16m106282x.
- [3] Álvaro Cartea, Sebastian Jaimungal, and Jason Ricci. “Buy low, sell high: A high frequency trading perspective”. In: *SIAM Journal on Financial Mathematics* 5.1 (Jan. 2014), pp. 415–444. DOI: 10.1137/130911196.
- [4] Martin D. Gould et al. “Limit order books”. In: *Quantitative Finance* 13.11 (Nov. 2013), pp. 1709–1742. DOI: 10.1080/14697688.2013.803148.
- [5] Jeremy Large. “Measuring the resiliency of an electronic limit order book”. In: *Journal of Financial Markets* 10.1 (Feb. 2007), pp. 1–25. DOI: 10.1016/j.finmar.2006.09.001.
- [6] Raman Uppal and Tan Wang. “Model misspecification and underdiversification”. In: *The Journal of Finance* 58.6 (Nov. 2003), pp. 2465–2486. DOI: 10.1046/j.1540-6261.2003.00612.x.

A Convex Penalty Function Experiments

$$l(q) = \begin{cases} \theta q, & \text{if } |q| \leq q_0, \\ \theta q \sqrt{2|q|q_0 - q_0^2}, & \text{if } |q| > q_0. \end{cases}$$

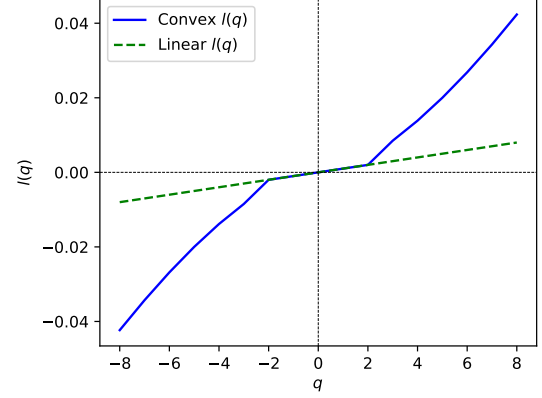


Figure 11: Definition of convex $l(q)$ and comparison with linear $l(q)$.

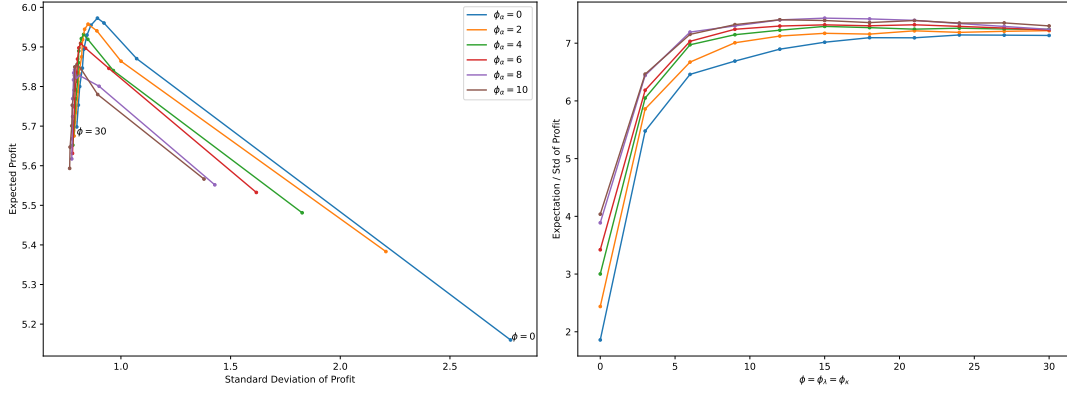


Figure 12: Expectation, standard deviation and Sharpe ratio of terminal wealth for various ambiguity parameters, 300 seconds of simulation under a convex $l(q)$, with $\theta = 0.001$ and $q_0 = 2$.